Supplemental Material for

Improving the accuracy of the sediment velocity structure obtained from the deep seismic sounding data by extracting multimodal dispersion curves

Wenbin Guo[1,2], Zhengbo Li[3,4] Shuai Zhao[5], Xiaofei Chen[3,4]

[1]School of Earth and Space Sciences, University of Science and Technology of China

[2]Geophysical Exploration Center, China Earthquake Administration

[3]Shenzhen Key Laboratory of Deep Offshore Oil and Gas Exploration Technology, Southern University of Science and Technology, Shenzhen, 518055, China

[4]Department of Earth and Space Sciences, Southern University of Science and Technology

[5]Beijing Earthquake Administration

Introduction

Figure s1-6 are the spectrograms extracted from SP11 data and SP15 data by phase slant stack method, phase shift method and original F-J method.

Figure s7 is the spectrograms extracted from SP14 data with original F-J method. Comparing the Figure s7 with Fig.5e-f in the main text, we could find that the spectrograms extracted from the seismic data in the same location, generated by different sources are similar to each other, further indicating accuracy of the spectrogram extraction.

Figure s8 presented the F-J spectrograms extracted from the synthetic seismic data that generated by the best fitting models with actual geometry.

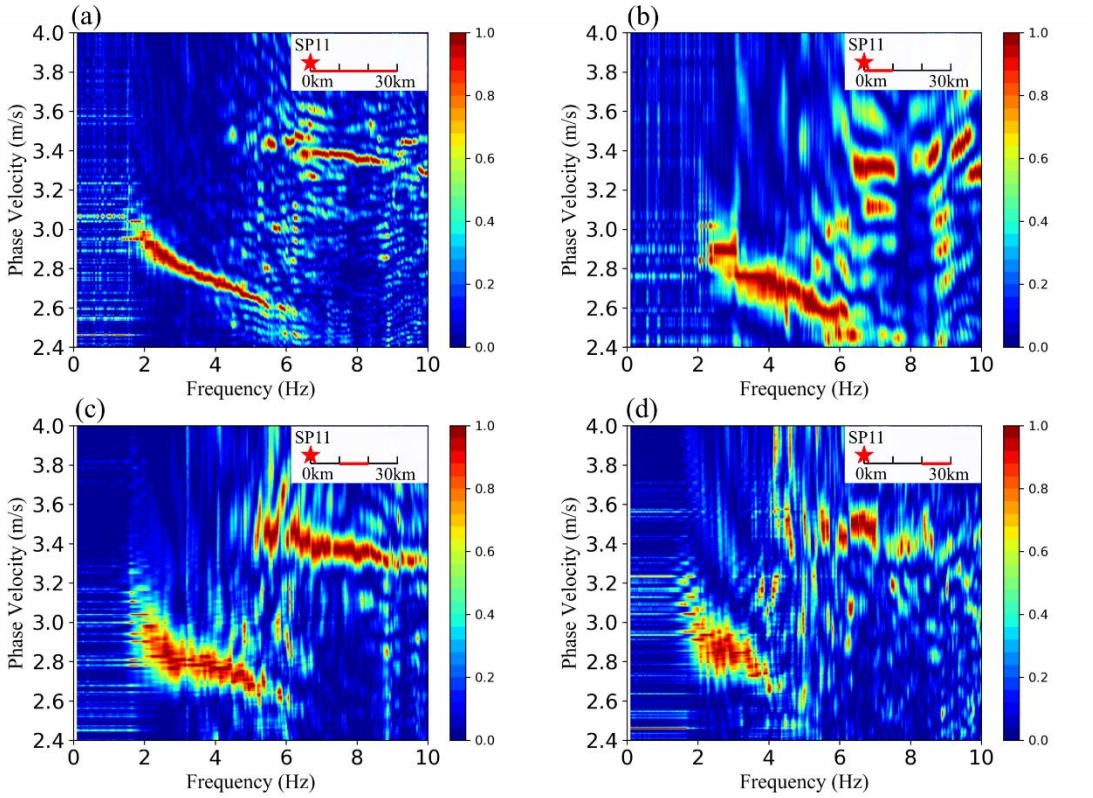

Figure s1. The spectrograms extracted from the SP11 data with phase slant stack method. (a) The spectrogram from 0 -30 km offset data. (b) The spectrogram from 0 - 10 km offset data. (c) The spectrogram from 10 -20 km offset data. (d) The spectrogram from 20 -30 km offset data.

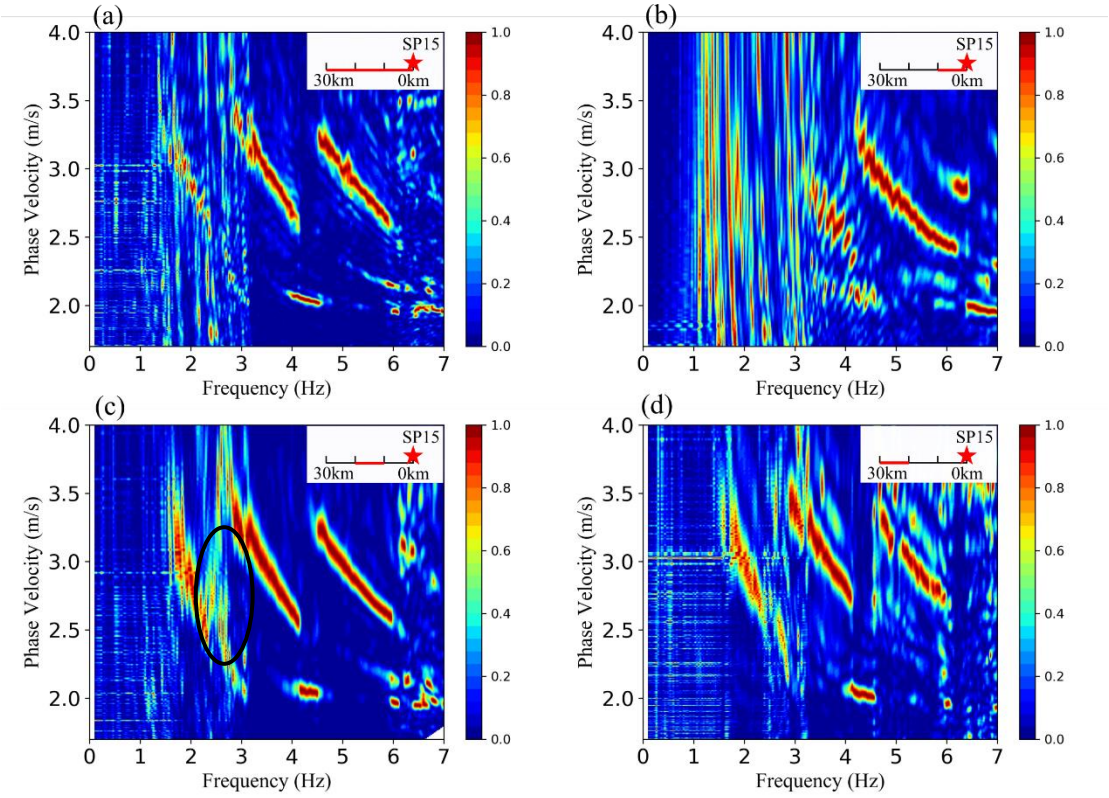

Figure s2. The spectrograms extracted from the SP15 data with phase slant stack method. (a) The spectrogram from 0 -30 km offset data. (b) The spectrogram from 0 -10 km offset data. (c) The spectrogram from 10 -20 km offset data. (d) The spectrogram from 20 -30 km offset data.

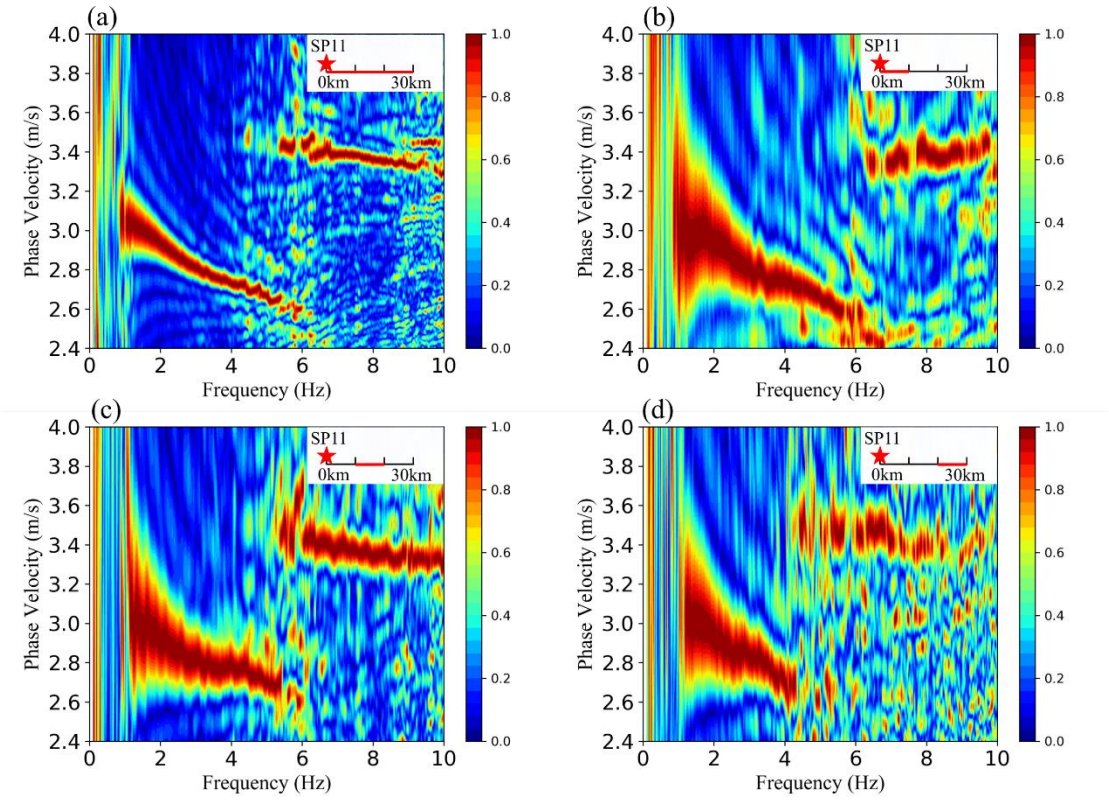

Figure s3. The spectrograms extracted from the SP11 data with phase shift method. (a) The spectrogram from 0 -30 km offset data. (b) The spectrogram from 0 -10 km offset data. (c) The spectrogram from 10 -20 km offset data. (d) The spectrogram from 20 -30 km offset data.

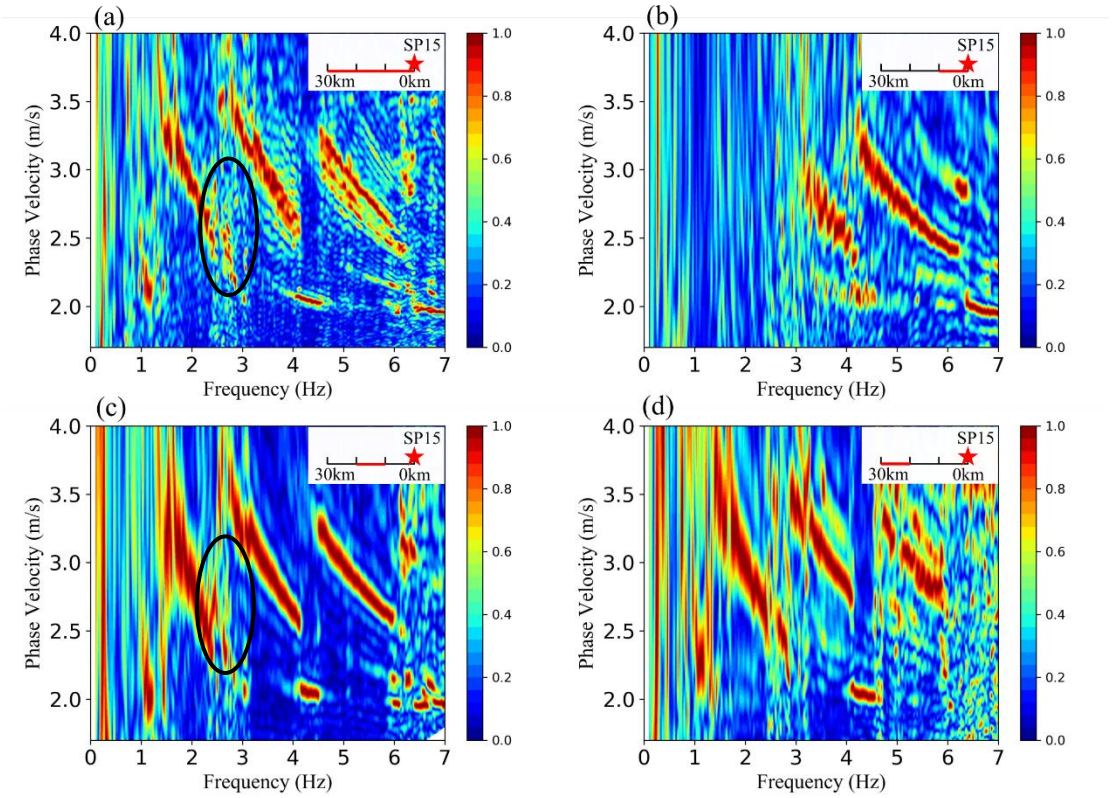

Figure s4. The spectrograms extracted from the SP15 data with phase shift method. (a) The spectrogram from 0 -30 km offset data. (b) The spectrogram from 0 -10 km offset data. (c) The spectrogram from 10 -20 km offset data. (d) The spectrogram from 20 -30 km offset data.

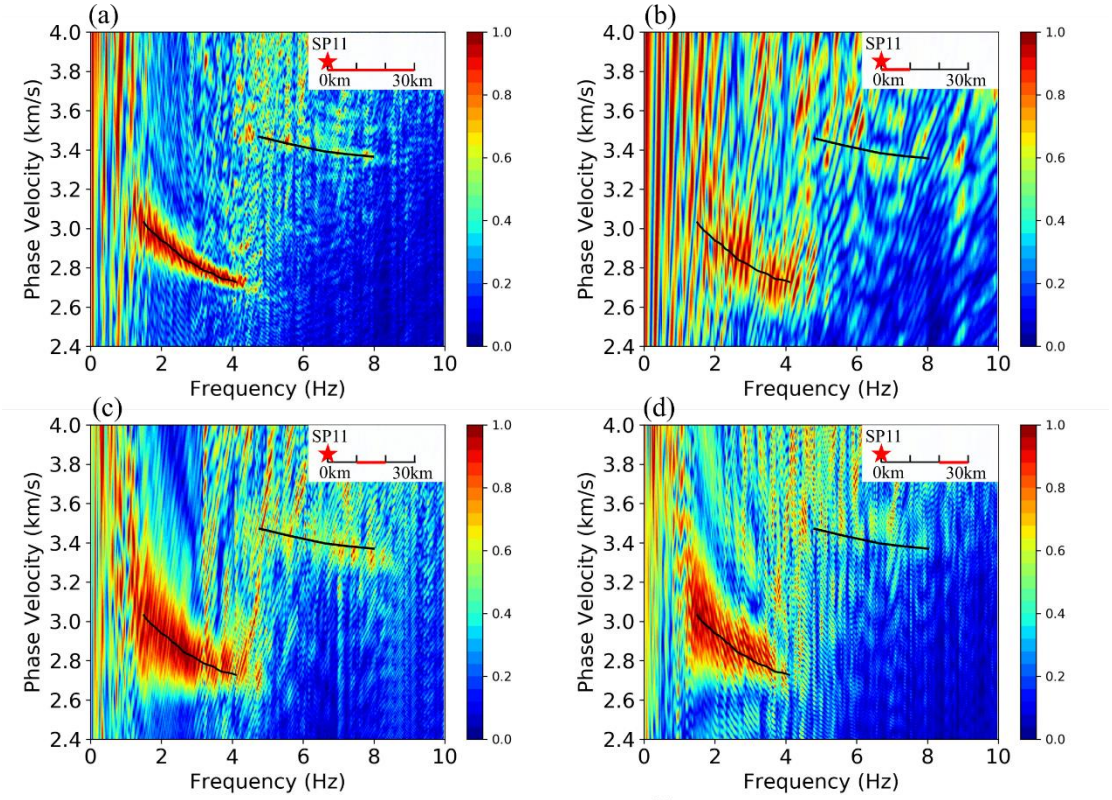

Figure s5. The spectrograms extracted from the SP11 data with the original F-J method. The black lines indicate the locations of the picked dispersion curves in Fig. 4a of the main text. (a) The spectrogram from 0 -30 km offset data. (b) The spectrogram from 0 -10 km offset data. (c) The spectrogram from 10 -20 km offset data. (d) The spectrogram from 20 -30 km offset data.

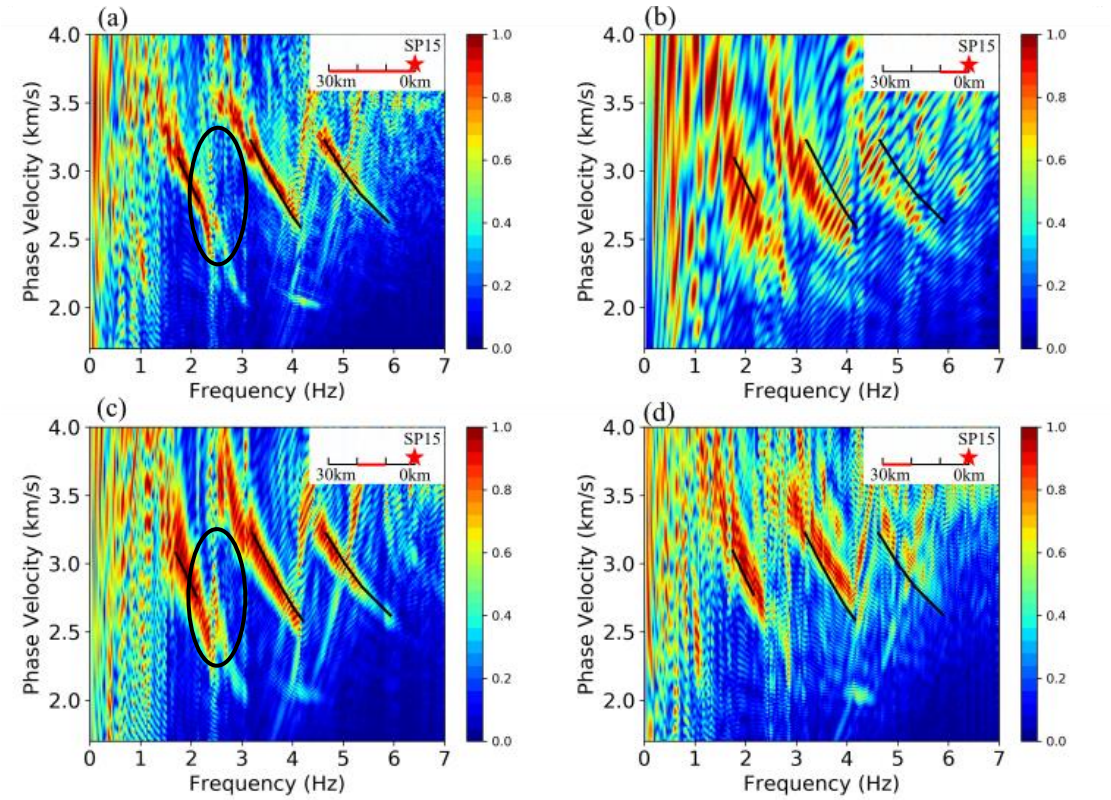

Figure s6. The spectrograms extracted from the SP15 data original F-J method. The black lines indicate the locations of the picked dispersion curves in Fig. 4b of the main text. (a) The spectrogram from 0 -30 km offset data. (b) The spectrogram from 0 -10 km offset data. (c) The spectrogram from 10 -20 km offset data. (d) The spectrogram from 20 -30 km offset data.

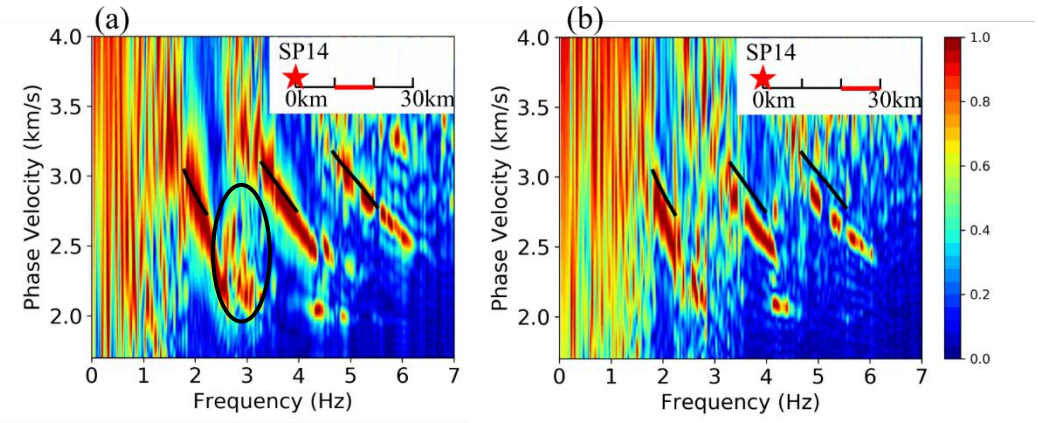

Figure s7. The spectrograms extracted from the SP14 data with F-J method. The black lines indicate the locations of the picked dispersion curves in Fig. 4b of the main text. The qualified spectrogram has not been extracted from the 0 -10 km offset. (a) The spectrogram from 10 -20 km offset data. (b) The spectrogram from 20 -30 km offset data.

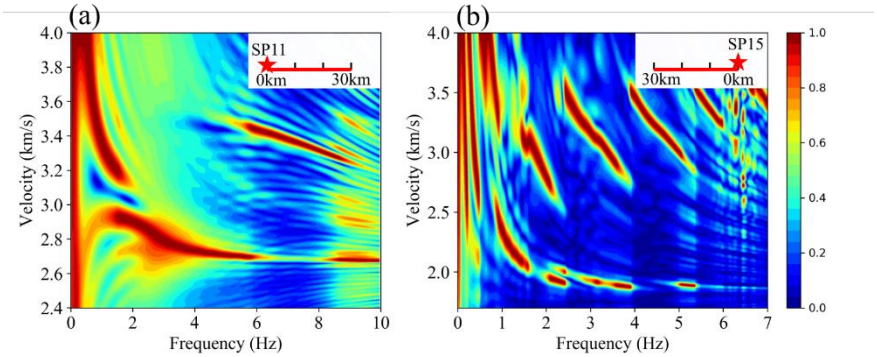

Figure s8. F-J spectrograms extracted from the synthetic seismic data. (a) The spectrograms of the synthetic seismic data generated by model 5 in Table 1. (b) The spectrograms of the synthetic seismic data generated by model 4 in Table 2.